ISSN 0020-4412, Instruments and Experimental Techniques, 2009, Vol. 52, No. 3, pp. 321–325. © Pleiades Publishing, Ltd., 2009.
Original Russian Text © A.A. Golubev, E.V. Gur'eva, A.V. Kantsyrev, V.A. Korolev, N.V. Markov, I.V. Rudskoi, G.N. Smirnov, V.I. Turtikov, A.D. Fertman, A.V. Khudomyasov, B.Yu. Sharkov, 2009, published in Pribory i Tekhnika Eksperimenta, 2009, No. 3, pp. 13–18.

NUCLEAR EXPERIMENTAL TECHNIQUE

Nonperturbing Gas Diagnostics of Ion Beams

A. A. Golubev, E. V. Gur'eva, A. V. Kantsyrev, V. A. Korolev, N. V. Markov, I. V. Rudskoi, G. N. Smirnov, V. I. Turtikov, A. D. Fertman, A. V. Khudomyasov, and B. Yu. Sharkov

Institute for Theoretical and Experimental Physics, ul. Bol'shaya Cheremushkinskaya 25, Moscow, 117218 Russia

Received October 6, 2008

Abstract—The usability of the gas scintillation method in almost nonperturbing diagnostics of ion beams was investigated. The width of the beam was measured on the ITEP–TWAC setup by its image in argon atmosphere at different gas pressures and beam intensities. The dependences of the luminescence intensity of argon atoms on the number of ions in a pulse and the gas pressure in the diagnostic chamber were obtained.

PACS numbers: 29.27.Fh, 29.40.Cs, 29.40.-n, 29.40.Rg

DOI: 10.1134/S0020441209030026

INTRODUCTION

Detailed information on the spatial distribution of particles in the beam transport channel and at the site of the experimental target is necessary for basic and applied research using ion beams; therefore, beam diagnostic systems are an integral part of almost any experiment at an accelerator. In recent years, different accelerator laboratories at GSI (Darmstadt, Germany), CERN, Sacle, and the Institute for Theoretical and Experimental Physics (ITEP; Moscow, Russia) have placed high emphasis on development of systems for nondestructive monitoring of intense charged particle beams [1–5].

The use of different techniques allows the characteristics of charged particle beams to be monitored in processes of their formation, acceleration, and transportation to an experimental setup. Nevertheless, available diagnostic methods (monitors based on residual gas ionization, multiwire proportional chambers, optical diagnostics, etc. [1]) permit measurements of the beam parameters only in one of the directions. When a beam possesses cylindrical symmetry, interpretation of experimental results creates no problems. However, in most cases, the beam has a more intricate shape and its profile cannot be reconstructed from experimental results obtained only in one direction.

In addition, in the majority of high-energy-density physics experiments, an intense ion beam is focused at the target into a spot with a diameter of several hundreds of microns. In this case, the transverse beam intensity distribution in the focal plane must be measured with a resolution of 10–50 μm. The basic factor that complicates such measurements is a high level of energy density in the detector material. Even when diagnostic tools perturb the beam only slightly (e.g., when multiwire scanners are used [1]), the detector material is heated to temperatures of 2000–5000 K. For example, experiments on the HHT setup at GSI have demonstrated that most materials (in particular, tungsten) melt or evaporate under the action of a single ion pulse [6–8]. Moreover, hydrodynamic expansion of the heated substance occurs as early as when the beam passes through the target (or the detector) and, therefore, the material density changes substantially during the interaction [9, 10].

This problem becomes more acute in future high-energy-density physics experiments on the FAIR facility for antiproton and ion research [11] proposed by the HEDgeHOB collaboration [12, 13]. The ion beam intensity on the new setup must be greater by at least two orders of magnitude than the values now attainable at the SIS-18 accelerator at the GSI.

In recent years, the potential of nonperturbing methods for diagnosing the spatial intensity distribution in high-power beams have been actively investigated. Among these methods are detection of the residual gas ionization and optical diagnostics of gas scintillations induced by transiting ions [14, 15]. By contrast to the other techniques, optical diagnostics allows simultaneous measurements of several beam projections in the same cross section of the channel, which helps reconstruct the beam profile of an intricate shape with a high degree of accuracy [16].

A set of experiments was carried out at the ITEP–TWAC accelerating–storage complex with the aim of investigating the physical fundamentals of the gas scintillation method [17]. The results of these studies are presented in this paper.

PHYSICAL FUNDAMENTALS OF THE METHOD

Determining the profile of the ion beam by the spatial distribution of the photon flux and the time variations in the radiation intensity forms the basis for the diagnostic method proposed in this paper. In this case,

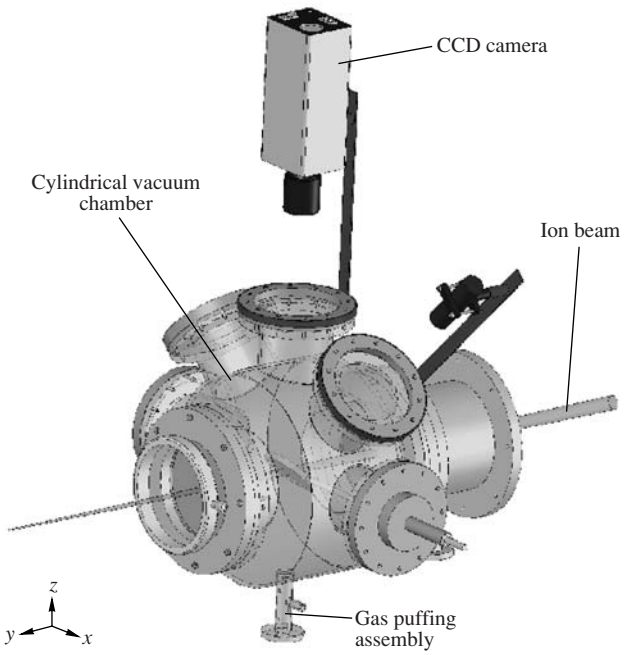

Fig. 1. Layout of the experiment.

the problem can be solved both by using special diagnostic chambers (with foil windows that limit the volume), which are filled with a gas to a pressure of 30–750 Torr and integrated into the ion guide, and by detecting luminescent emission of the residual gas components. However, the residual gas pressure must not be lower than 10^{-8} Torr even when high-intensity beams are detected; otherwise, luminescent emission will be extremely weak and, therefore, undetectable.

Deceleration by ionization is the main energy loss mechanism when a charged particle moves through the gas that fills the diagnostic chamber. An ion traveling through the gas suffers Coulomb interaction with electrons and spends part of its energy on excitation and ionization of atoms in the medium. The inner energy levels are deexcited by emission of a photon. We assume that the luminescent emission intensity is directly proportional to the number of particles in the beam. However, passing of an ion beam through the gas is followed by production of numerous secondary electrons, which can leave the region of primary interaction between ions and the substance and also excite and ionize gas atoms. This process may cause the luminescent region to broaden and distort the image in comparison with the actual ion beam profile [18]. In addition, in practice, detected luminescent emission of the gas excited by an ion beam depends both on the primary interaction of ions with the substance and on subsequent interactions with gas atoms. Nonradiative quenching of excited states, photoeffect, Compton effect, and other phenomena should also be taken into account.

EXPERIMENTAL SETUP

To test the proposed technique, a stainless steel cylindrical vacuum chamber (Fig. 1) has been produced by the ITEP. The chamber has been designed so that luminescent emission of a gas can be observed from five different directions. The chamber is located at the end of the beam transport line and separated from the high-vacuum channel by a composite foil. The chamber can be pumped down to a pressure of 10^{-4} Torr and filled with various gases.

Systematic measurements of the luminescence intensity of argon were taken on the ITEP terawatt accumulator (ITEP–TWAC) at different gas pressures in the diagnostic chamber. The layout of the experiment is shown in Fig. 1. A beam of C^{6+} ions with an energy of 216 MeV/amu was used in the study. Two 20K100 quadrupole lenses maintained sharp beam focusing onto the gas-filled diagnostic chamber.

The cylindrical chamber volume is 300 mm in diameter; its length downstream of the beam is 160 mm. The entrance and exit flanges of the chamber are closed with diaphragms; the diameter of the entrance and exit windows is 150 mm. The base material of the diaphragms is 108-μm-thick kapton ($C_{22}H_{10}N_2O_5$, d = 1.42 g/cm^3). The kapton is coated on two sides by a 10-μm-thick copper layer, two nickel layers 10 μm thick each, and two gold layers 0.43 μm thick each. Five glass windows equipped with flange joints are mounted around the periphery of the cylinder at different angles in a plane perpendicular to the beam. These windows are either light-insulated or used in accordance with the experimental tasks. Argon was used in the experiments as a working gas.

A fast current transformer (Bergoz [19]) was placed directly behind the exit window of the chamber (downstream of the beam). This transformer was used to measure the time profile of the beam (an example in Fig. 2) with a nanosecond resolution and determine the total number of particles in the ion beam pulse. The pulse duration at its base was ≈800 ns.

The number of particles in a beam pulse was varied from 1.5×10^8 to 3.5×10^9 ions/bunch. To measure the number of particles in a pulse, the beam was spilled at different ion stacking levels in the accelerator ring.

Ion-beam-induced light emission of the scintillator was detected by an SDU-285 CCD camera [20]. The camera was installed in a plane perpendicular to the beam (see Fig. 1) and equipped with optical devices providing a field of vision of ~5 cm. The coefficient of transmission of an image from the actual plane to the plane of the CCD array was 19.5 pixels/mm [20].

RESULTS OF MEASUREMENTS

Since, in our case, the extracted beam of carbon ions has a low intensity and heats the material during interaction with it only slightly, we use a plastic scintillator as a reference detector for determining the geometric

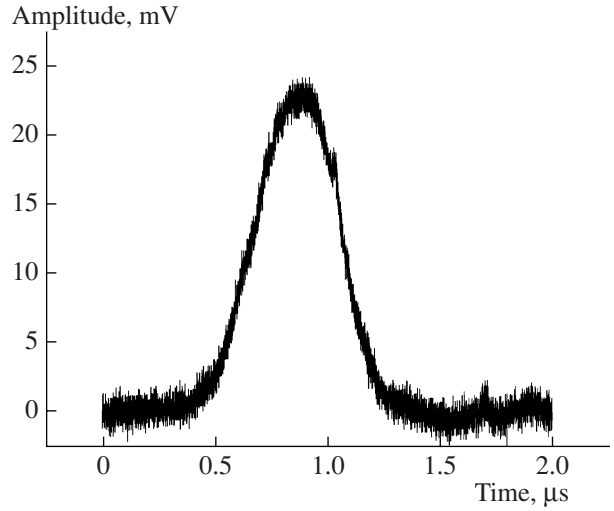

Fig. 2. Characteristic pulse shape of the carbon beam current.

characteristics of the beam. A vacuum-tight feedthrough was inserted into one of the windows of the diagnostic chamber and used to move an object inside the chamber without breaking the air tightness. A 1.5-mm-thick plate of Bicron-412 scintillator was fixed in place in a rectangular frame at the end of the vacuum-tight feedthrough rod and placed at the center of the vacuum volume at an angle of 45° both with the beam direction and with the direction of observation. Adjustment of the channel parameters and extraction of ions into the diagnostic chamber were performed using the beam image on the plastic scintillator. We decided to use a beam with a transverse dimension of ~2 mm to investigate gas scintillations induced by passing ions. At an available resolution, this allowed us to obtain >50 digitization points on a beam image.

During experimental investigations, the gas pressure in the diagnostic chamber was varied from 35 to 500 Torr. The profiles of the intensity distribution in a beam cross section were determined from the obtained images (Fig. 3). Figure 4 presents the typical profiles of scintillations in argon at a pressure of 500 Torr and the Bicron-412 plastic scintillator, which were recorded by the camera placed above the beam axis. It is apparent that these profiles coincide with a high degree of accuracy.

By processing the experimental data, we obtained the dependences of the gas scintillation intensity induced by the carbon beam on the number of particles in a beam pulse for different argon pressures in the diagnostic volume. Examples of these dependences are presented in Fig. 5. The results obtained for different gas pressures can be fitted by linear functions. Determining the slope angle of each straight line, we actually find the average value of the specific light yield (per single ion). The dependence of this quantity on the

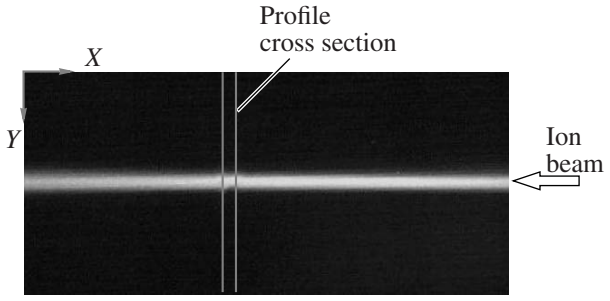

Fig. 3. Luminescent emission of argon induced by the carbon ion beam; the image was recorded by the SDU-285 CCD camera.

argon pressure in the diagnostic chamber is presented in Fig. 6.

The dependence of the average full width at half-maximum of the scintillation profile on the gas pressure is shown in Fig. 7. It is apparent that this parameter is almost independent of the pressure (in the range of 1.5×10^8 to 3.5×10^9 ions/bunch). The average width is 1.8 ± 0.2 mm; within the limits of the measurement error, this value coincides with the full width at half-maximum (FWHM) of 1.9 ± 0.1 mm obtained using the Bicron-412 plastic scintillator.

DISCUSSION OF THE RESULTS

The experimental data suggest that the dependence of the luminescent emission intensity in argon on the number of carbon ions is linear at pressures of 35–500 Torr and a beam intensity ranging from 1.5×10^8 to 3.5×10^9 ions per pulse with a duration of 1 μs (at the base).

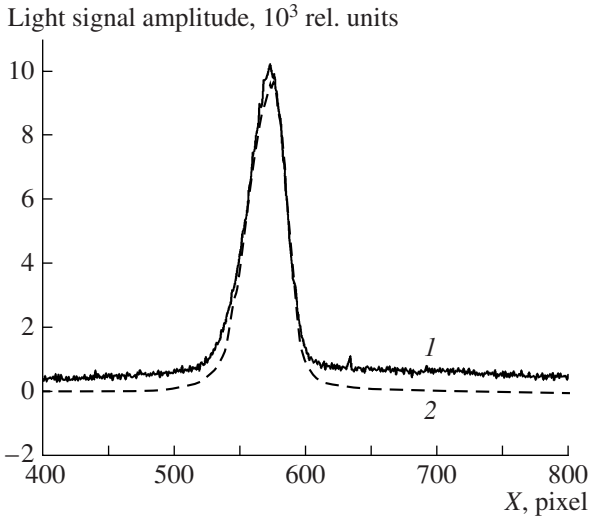

Fig. 4. Typical profiles of scintillations (*1*) in argon at a pressure of 500 Torr and (*2*) Bicron-412 plastic scintillator.

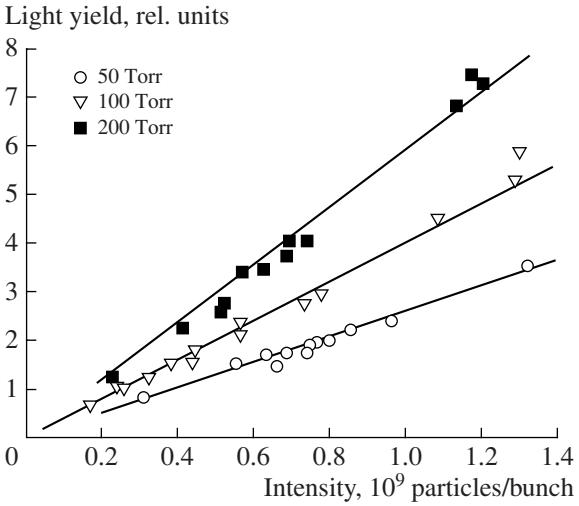

Fig. 5. Experimental dependences of the light yield in argon on the number of carbon ions in a beam pulse and their linear approximations at different argon pressures in the diagnostic chamber.

Within the limits of the experimental error, the width of the beam profile measured by its image in the gas is independent of the pressure in the diagnostic volume and the number of ions in a pulse in the investigated ranges of the gas pressure and beam intensity.

The behavior of the specific light yield on the gas pressure was found to be nonlinear (see Fig. 6). Such a behavior has already been observed in the earlier studies [21, 22] and explained by an increase in the probability of collision (i.e., nonradiative) quenching of excited states with an increase in the gas density. In fact, in the presence of nonradiative deexcitation channels, the light emission intensity in transition $n \longrightarrow k$ is defined by the expression

$$I \sim n_g \frac{A_{nk}}{A_{nk} + n_g \sum_i \langle v\sigma_i \rangle} \sim \frac{n_g}{1 + n_g \sum_i \langle v\sigma_i \rangle / A_{nk}}, \quad (1)$$

where A_{nk} is the probability of the radiative transition $n \longrightarrow k$, n_g is the gas density, $\sigma_i = \sigma_i(v)$ is the cross section of collisional quenching of a particular line in the ith channel, v is the relative velocity of colliding gas atoms, and angular brackets denote averaging over the velocity.

Unfortunately, the low intensity of the ion beam has made it impossible in our study to measure the spectral composition of detected radiation. Therefore, the available experimental data allow only a coarse estimation of the total cross section for collisional deexcitation of the ArI lines. Approximation of the experimental results by function (1) provides the best fit at $\sum_i \langle v\sigma_i \rangle / A_{nk} \approx 1.73 \times 10^{-19}$ (a solid line in Fig. 6). Taking into account the spectral response of the used

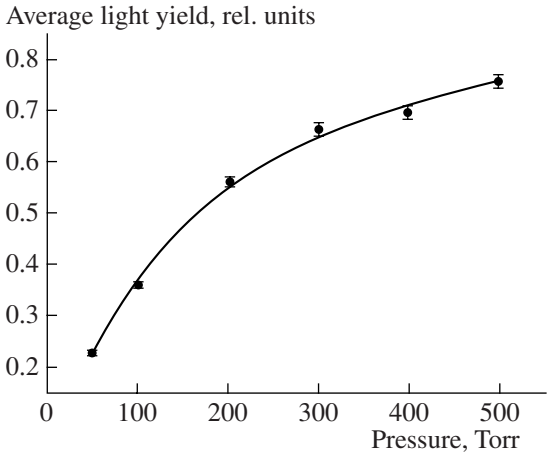

Fig. 6. Dependence of the specific light yield on the argon pressure.

camera [20], we can assume that the main contribution to the total luminescence intensity is made by the most powerful short-wave ArI lines $3p^5 4p \longrightarrow 3p^5 4s$, for which the mean probability of radiative transition is $\sim 4 \times 10^7$ s^{-1} [23]. From this, it follows that the total cross section of collisional transitions resulting in deexcitation can be estimated as

$$\bar{\sigma} \approx 1.73 \times 10^{-19} A_{nk}/v_t \approx 1.76 \times 10^{-16} \text{ cm}^2.$$

(In this formula, mean thermal velocity v_t of Ar atoms at normal temperature is assumed to be $\sim 3.94 \times 10^4$ cm/s.) The respective mean decay rate of excited states k is $\sim 2.3 \times 10^5$ s^{-1} Torr^{-1}, i.e., $\sim 1.9 \cdot 10^3$ s^{-1} Pa^{-1}. Similar results—$k \approx (3.16\text{–}4.24) \times 10^3$ s^{-1} Pa^{-1} for the shortest-wave lines—were obtained in [21], in which time-resolving measurements of the emission spectrum of argon excited by 15-MeV α particles were taken.

Agreement as good as this is also observed for normalized (on a per-atom basis) luminescence intensity,

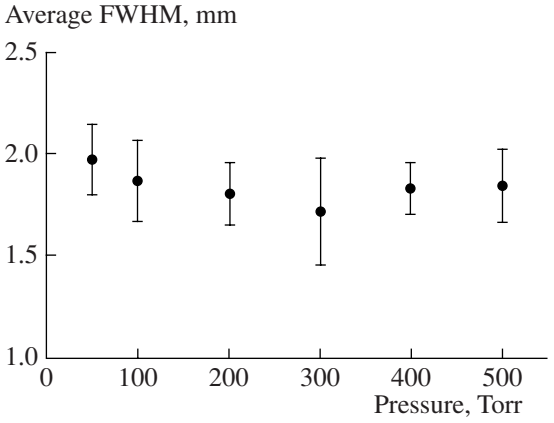

Fig. 7. Dependence of the average full width at half-maximum of the scintillation profile on the argon pressure.

which decreases with in increase in the gas pressure. In our study, this value is ~0.42 at a gas pressure varying from 75 to 450 Torr, which is very close to the mean value of 0.4 obtained in [21]. The small discrepancies can apparently be attributed to the abnormal behavior of transition $2p_2$ with a wavelength of 696.5 nm (an increase in the normalized intensity with pressure rise, $k \approx 0.18 \times 10^3$ s^{-1} Pa^{-1}), which makes a certain contribution to the spectrum-integral measurements performed in this study.

CONCLUSIONS

Our investigations showed that, for carbon beams with an intensity of up to 3.5×10^9 ions/bunch and a duration (at the base) of 1 μs, the image profiles obtained using the gas scintillation method agree with the profiles recorded with the aid of scintillating screens (the full widths of the profiles at half-maxima coincide within the limits of experimental errors). This allows us to propose using this technique as a diagnostic tool for this type of charged particle beams. Being almost nonperturbing, this diagnostics can be considered an alternative to the traditional techniques and, in addition, may turn out to be indispensable in experiments in which continuous beam monitoring is required.

ACKNOWLEDGMENTS

We thank V.K. Lebedev, V.V. Timofeev, and S.P. Shuvalov for their invaluable help in developing the beam transport channel; we also thank O.Yu. Zhiryakova for her help in the organizational management.

This work was supported by Rosatom, the Russian Foundation for Basic Research (project no. 07-02-13658-ofi_ts), the International Science and Technology Center (project no. 3591), and GSI-INTAS (project nos. 03-54-4254 and 06-10000128707).

REFERENCES

1. Forck, P., *Lectures Notes on Beam Instrumentation and Diagnostics. GSI*, Darmstadt, Germany: Joint University Accelerator School, 2006, p. 39.
2. Roudskoy, I.V., Golubev, A.A., Fertman, A.D., et al., *Laser and Part. Beams*, 2005, vol. 23, p. 539.
3. Artemov, A.S., Astrakharchik, G.F., Baigachev, Yu.K., and Gevorkov, A.K., *Zh. Tekh. Fiz.*, 2000, vol. 70, no. 1, p. 117 [*Tech. Phys.* (Engl. Transl.), vol. 70, no. 1, p. 116].
4. Burtin, G., Camas, J., Ferioli, G., et al., *Proc. of the 7th Eur. Part. Accel. Conf. (EPAC-2000)*, Vienna, 2000, vol. 1, p. 256; http://accelconf.web.cern.ch/AccelConf/e00/PAPERS/TUOAF103.pdf
5. Artemov, A.S. and Afanas'ev, S.V., *Fiz. Elem. Chastits At. Yadra*, 2006, vol. 37, no. 4, p. 983 [*Phys. Part. Nucl.* (Engl. Transl.), vol. 37, no. 4, p. 520].
6. Ni, P., Hoffmann, D.H.H., Kulish, M., et al., *Journal de Physique IV*, 2006, vol. 133, p. 977.
7. Udrea, S., Ternovoi, V., Shilkin, N., et al., *Nucl. Instrum. Methods Phys. Res. A*, 2007, vol. 577, p. 257.
8. Varentsov, D., Ternovoi, V.Y., Kulish, M., et al., *Nucl. Instrum. Methods Phys. Res. A*, 2007, vol. 577, p. 262.
9. Varentsov, D., Spiller, P., Fank, U.N., et al., *Nucl. Instrum. Methods Phys. Res. B*, 2001, vol. 174, p. 215.
10. Varentsov, D., Tahir, N.A., Lomonosov, I.V., et al., *Europhys. Lett.*, 2003, vol. 64, p. 57.
11. Henning, W.F., *Nucl. Instrum. Methods Phys. Res. B*, 2003, vol. 204, p. 725.
12. *HEDgeHOB Collaboration. Technical Report for HEDgeHOB Collaboration Experiments / FAIR Baseline Technical Report. GSI*, H.H. Guthbrod, Ed., Darmstadt, Germany, 2006, vol. 5; http:/www.gsi.de/reports/btr.html
13. Hoffman, D.H.H., Fortov, V.E., Lomonosov, I.V., et al., *Physics of Plasmas*, 2002, vol. 9, p. 3651.
14. Variola, A., Jung, R., and Feroioli, G., *Phys. Rev. ST Accel. Beams*, 2007, vol. 10, p. 122801.
15. Becker, F., Hug, A., Fork, P., et al., *Laser and Part. Beams*, 2006, vol. 24, p. 541.
16. Belyaev, G., Roudskoy, I., Gardes, D., et al., *Nucl. Instrum. Methods Phys. Res. A*, 2007, vol. 578, p. 47.
17. Sharkov, B., Alexeev, N.M., Churazov, M.D., et al., *Nucl. Instrum. Methods Phys. Res. A*, 2001, vol. 464, p. 1.
18. Gardes, D., Ausset, P., Bousson, S., et al., *GSI Report*, 2001, no. 97-08, p. 47.
19. http:/www.bergoz.com/products/FCT/d-fct.html
20. *Tsifrovaya kamera SDU-285. Tekhnicheskoe opisanie (firmware Ver. 1.03)* (SDU-285 Digital Camera: Instruction Manual (Firmware Ver. 1.03)), OOO Spetsteletekhnika, 2007; www.sptt.ru
21. Aho, K., Lindblom, P., Olsson, T., et al., *J. Phys. B*, 1998, vol. 31, p. 4191.
22. Gardes, D., Maynard, G., Belyaev, G., et al., *Nucl. Instrum. Methods Phys. Res. B*, 2001, vol. 184, p. 458.
23. Wiese, W.L., Brault, J.W., Danzmann, K., et al., *Phys. Rev. A*, 1989, vol. 39, p. 2461.